Influence of hot isostatic pressing on the properties of 316L stainless steel, Al-Mg-Sc-Zr alloy, titanium and Ti6Al4V cold spray deposits

P. Petrovskiy, M. Khomutov, V. Cheverikin, A. Travyanov, A. Sova, I. Smurov

Influence of hot isostatic pressing on the properties of 316L stainless steel, Al-Mg-Sc-Zr alloy, titanium and Ti6Al4V cold spray deposits

P. Petrovskiy[a], M. Khomutov[a], V. Cheverikin[a], A. Travyanov[a], A. Sova[b], I. Smurov[a, b]

a - National University of Science and Technology "MISiS", 4 Leninsky prospect, 119991, Moscow, Russia

b - Lyon University, ENISE, LTDS Laboratory, UMR CNRS 5513, 58 rue Jean Parot, 42023, Saint-Etienne Cedex 2, France

Abstract

In this paper an effect of capsule-free hot isostatic pressing (HIP) on the porosity and mechanical properties of different cold spray deposits was experimentally evaluated. The HIP post-treatment significantly decreased (more than 2 times) the porosity of 316L and pure titanium deposits. The densification effect of HIP on the porous Ti6Al4V deposit was significantly less pronounced. Mechanical properties of the deposits after HIP were also improved. In particular, the tensile strength of the stainless steel, pure titanium and Ti6AL4V increased from 30 MPa, 70 MPa and 20 MPa to 211 MPa, 480 MPA and 560 MPa correspondingly. Compressive strength of the Al-Mg-Sc-Zr alloy samples after HIP was also increased ~25%. Improvement of mechanical properties is explained by material diffusion and microstructure changes during HIP cycle.

Keywords: cold spray, hot isostatic pressing, stainless steel, titanium, aluminum alloy

Introduction

Cold gas dynamic spray is a solid-state process used for metal coating deposition as well as for additive manufacturing [1-6]. In this process, the particles of deposited material are accelerated and heated by supersonic gas flow in converging-diverging nozzle. If the particle impact velocity exceeds certain critical value, the particle deformation at impact leads to formation of metal jets at the particle / substrate interface. Jet formation provokes the rupture of thin oxide films on the substrate and particle surfaces that allows establishing close contact between two chemically active metal surfaces. As a consequence strong bonding between two materials could be achieved. [1, 7-10].

In general, the mechanical properties of cold spray deposits are lower than the reference values obtained for bulk materials. In particular, it is known that the cold spray coatings and spray formed 3D objects have low ductility [5, 10-14]. The ultimate tensile strength of the deposits strongly depending on the powder properties and spraying parameters may vary from 5% to 100% relatively the reference values of UTS [5, 10]. Low ductility and significant variation of UTS is explained by the specific structure of the deposits. The cold spray deposit consist of severely deformed metal particles (splats). The TEM and SEM observations of the splat cross-section revealed very fine microstructure [10]. Such grain refinement is explained by intensive plastic deformation during impact. As a consequence, the ductility of splat is limited whereas the hardness is elevated. The second and the most important factor determining the brittle behavior of cold spray deposits is the quality of the contact between splats. As it was reported in many articles, the main mechanism of the coating failure generally observed during tensile test is the fragile rupture at the splat interface [11, 13-16]. Poor material bonding at the splat interface is generally explained by insufficient material diffusion between two connected surfaces. Third factor diminishing the mechanical performance of cold spray deposits is the coating porosity. The previous studies showed that two types of the cold spray coating porosity could be introduced [17, 18]. Porosity of the first type depends on the efficiency of the particle deformation at impact. In case of insufficient deformation the particle material is not capable to fill the asperities on the impacted surface. These gaps located at the splat interfaces and limiting the intersplat contact area represent the porosity of the first type. The pores of second type are located at the interfaces between connected coating lines and superposed coating layers. In this case the pores are formed due to unfavorable particle impact angle at the slopes of the coating lines. The porosity of the second type could be controlled by proper selection of the nozzle displacement strategy in order to avoid the formation of thick coating lines with high slope angle.

Ductility and UTS of cold spray deposits can be increased by application of heat-treatment after spraying [13]. Heat treatment intensifies the material diffusion between the splats and leads to material recrystallization at the splat interface. As a result, the joint grains between the splats could be formed [11-14, 19]. Also, the heat treatment contributes to the grain growth inside the splats that increases material ductility [10]. At the same time, the heat treatment has limited effect on the coating porosity. As a consequence, even recrystallized coatings could have low UTS and ductility due to elevated residual porosity [13].

In this regard, the hot isostatic pressing (HIP) of cold-sprayed deposits could be considered as a promising post-treatment method providing combined effect: material

recrystallization and material densification. In this process, the high pressure caused by hot pressurized gas around the part affects the stress around a single pore, inducing pore shrinkage and accelerating the diffusion of material [20, 21]. Nowadays two types of HIP are used: pressing within deformable metal capsules and capsule-free pressing (Figure 1) [20, 21].

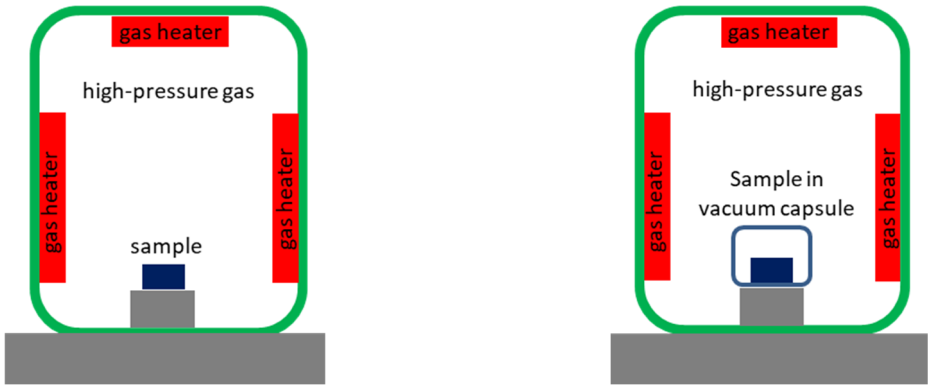

Figure 1: Schematic illustration of capsule-free (a) and encapsulated (b) hot isostatic pressing (HIP)

In capsule-free HIP the part is placed in direct contact with the hot pressurized inert gas inside the HIP chamber. The hot and dense gaseous environment inside the chamber induces gas absorption by the pore walls inside the treated part, followed by pore shrinkage. However, in case of high open porosity, the capsule-free HIP cannot provide material densification owing to gas transfer between connected pores and the surface of the part. In this case, hot isostatic pressing within deformable capsules (encapsulated HIP treatment) can be applied. During encapsulated HIP, the part is closed in sealed metal capsule. The gas inside the capsule is removed by a vacuum pump before the capsule is placed inside the HIP chamber. The gas trapped inside the open pores is also removed during capsule vacuuming. The gas pressure causes capsule wall shrinkage during HIP [20, 21].

In powder-bed additive manufacturing the capsule-free HIP is applied for densification of manufactured parts [22-25]. The application of encapsulated HIP is significantly less common due to expensive procedure of part encapsulation and vacuuming. In contrast to powder bed additive manufacturing methods, only few papers devoted to the application of HIP for improvement of cold spray coating or 3D part structure could be find in the literature [26-30]. HIP treatment of cold-sprayed titanium alloys was first reported by Blose et al. [26]. Unfortunately, the authors did not specify which type of HIP treatment was applied (encapsulated or capsule-free). Detailed description of HIP parameters was not provided. However, the authors reported significant improvement of the coating density after hot isostatic

pressing. In recent work Chen et al. performed a comprehensive study of the effects of capsule-free HIP on the properties of nitrogen-sprayed and helium-sprayed Ti6Al4V cold-sprayed deposits [27]. The HIP allowed to increase the UTS of nitrogen-sprayed and helium-sprayed samples from ~100 to ~650 MPa and from ~380 to 950 MPa, respectively. Chen et al. concluded that capsule-free HIP cannot increase the UTS of nitrogen-sprayed samples to those of bulk material owing to poor pore elimination. Yin at al. [28] reported significant improvement of stainless steel coating porosity after capsule-free HIP. Although the deposit porosity was significantly reduced after HIP treatment, the mechanical properties did not surpass the vacuum-annealed samples. Authors considered that it may be caused by the original oxide films retained at the particle surfaces in the original inter-particle pore areas, effectively hindering the intimate metallurgical inter-particle bonding even after the pores collapse in HIP [28].

In contrast to vacuum heat treatment or heat treatment in neutral gas environment, the application of HIP as post-processing procedure of cold spray deposits is a relatively new approach capable of improvement the material density and the mechanical properties. It is important to note, that at present no recommendations for the optimal HIP treatment parameters of cold spray deposits are presented in the literature. In this paper the first results of several feasibility studies devoted to the application of capsule-free HIP for improvement of the mechanical properties and density of different cold spray deposits are presented.

Materials and methods

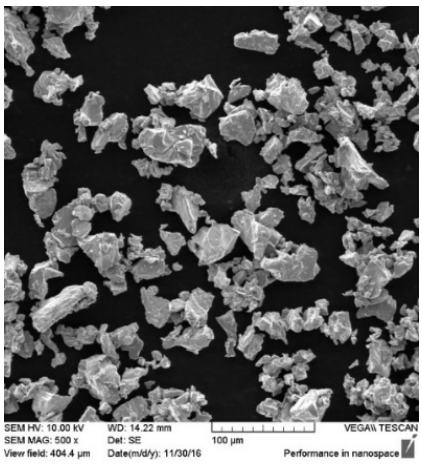

a

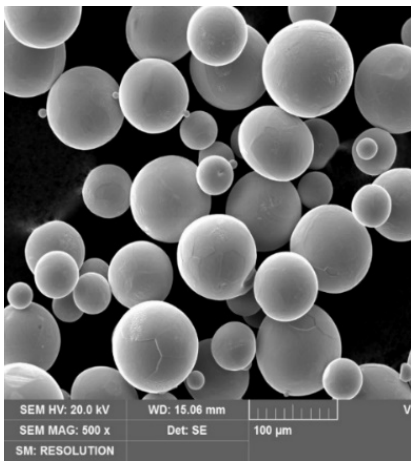

b

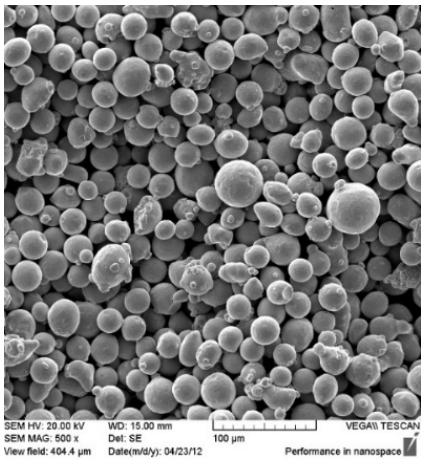

c

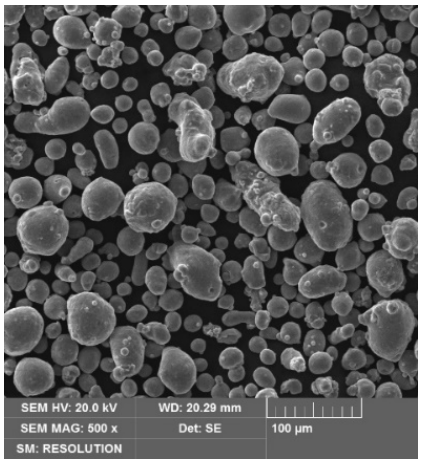

d

Figure 2 : SEM images of powers: (a) – titanium, (b) - Ti6Al4V alloy, (c) - 316L stainless steel, (d) - Al-Mg-Sc-Zr alloy

Four powders were used in this study: commercially available 316L austenitic stainless steel (Sandvik Osprey), commercially available pure titanium (Stark, Amperit 155.054), Ti6Al4V produced at MISIS University (Moscow, Russia) by gas-atomization and commercially available Al-Mg-Sc-Zr (Rusal, RS-553, UC). The SEM mages of the powders are presented in Figure 2. The particle size distributions measured by Occhio ALPAGA 500 optical granulomorphometer are presented in Table 1.

Table 1: Particle size distribution of powder used in experiments.

Material	*D10, µm*	*D50, µm*	*D90, µm*
Titanium	15	20	46
Ti6Al4V	11	52	95
SS 316L	5	27	35
Al-Mg-Sc-Zr	10	33	52

The samples were produced using commercial cold spray equipment Impact 5/8 (Impact Innovations, Germany) with the OUT-1 nozzle [40]. The spraying gun was fixed during deposition and the substrate was displaced by a six-axis robot (KUKA, Germany). Nitrogen was applied as the working gas and powder carrier gas. In all cases the spraying was performed on aluminum plates sandblasted using mesh 120 alumina grains. Spraying parameters are specified in Table 2. In all cases the substrate displacement velocity was adjusted in order to obtain the coating line with the thickness near 0.4 - 0.5 mm per pass. The hatch distance between coating lines was 3 mm. The final deposits with approximate dimensions 60 × 60 mm and the thickness ~40 mm (ten coating layers) were produced. Two batches of samples were manufactured for each powder. The deposits were separated from the substrate by electrical discharge machining. The samples in the first batch underwent capsule-free HIP, whereas those in the second batch were analyzed in the as-sprayed condition.

Table 2: Spraying parameters

Material	*Gas pressure, bars*	*Gas temperature, °C*	*Substrate displacement speed, mm/s*
Titanium	40	800	50
Ti6Al4V	40	800	50
SS 316L	40	650	50
Al-Mg-Sc-Zr	40	350	25

The capsule-free hot isostatic pressing of the samples was conducted in argon atmosphere using the HIRP70/150-200-1300 equipment produced by ABRAAG (Switzerland). The HIP parameters are provided in Table 3. Taking into account the absence of available data about the optimal HIP parameters of cold spray deposits, the standard HIP parameters typically used for HIP treatment of powder-bed laser fusion 3D parts were used.

Table 3: HIP parameters used for sample treatment

Material	*Pressure*	*Temperature*	*Time*
Titanium	150 MPa	900 °C	3h
Ti6Al4V	150 MPa	910 °C	2h
SS 316L	150 MPa	1050 °C	2h
Al-Mg-Sc-Zr	160 MPa	300°C + 360°C	3h+4h

Both batches of samples were subjected to metallographic preparation procedure. The sample microstructure was analyzed using an optical microscope (Olympus BX51, Olympus, Japan) and a scanning electron microscope (Vega 3LMH, Tescan, Czechia). Porosity measurements of all samples were performed using optical images obtained by Carl Zeiss Axiovert 200M MAT (Carl Zeiss, Germany) optical microscope. The images were treated by AxioVision 4.5 software developed for porosity measurement. The porosity of Ti6Al4V and 316L coatings were also measured using X-ray tomographic scanner XT H 225 ST Nikon Metrology with the open-type micro-focus X-ray tube with the maximum power of 225 kW, rated power of 225 W and the focal spot size of 3 µm.

Tensile tests were performed for pure titanium, Ti6Al4V and 316L stainless steel in accordance with the ASTM E-8 standard. The tensile samples were cut by electrical discharge machining. The dimensions of samples are presented in Figure 3. The strain direction during tensile testing was parallel to the nozzle pass direction. Twelve tensile samples were produced for each material: six for the as-sprayed coating and six for the coating after HIP treatment. Compression tests were carried out with the Al-Mg-Sc-Zr samples. Compression tests as well as the tensile tests were performed using Zwick Z250 (ZwickRoell, Germany) universal testing machine. The compression test were performed on the cylindrical samples 1.2 mm in diameter and 2.5 mm in height with deformation rate of 4 mm/min. The axis of the cylinders were

perpendicular to the substrate. Cut pattern of the tensile and compression test samples is presented in Figure 3.

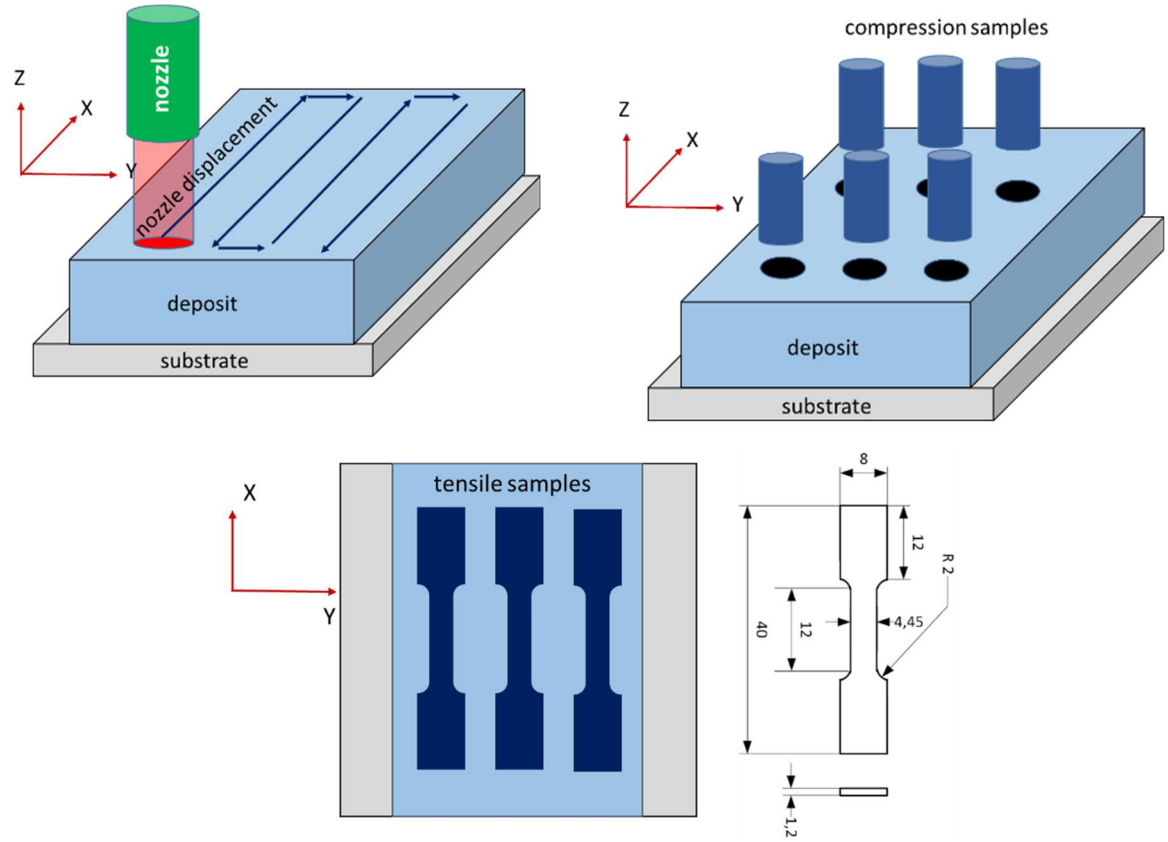

Figure 3: Cut pattern of the tensile and compression test samples

Results and discussion

Structure and porosity

The SEM images of coating cross-sections in as-sprayed conditions are presented in Figures 4-7. No macro-defects or cracks were detected. All coatings had typical splat structure. The boundaries between splats are well visible on the images. Higher magnification images revealed the zones with close contact between the splats boundaries as well as the zones with the defects and poorly bonded splats. The pores located at the splat interfaces are well visible on the images. The pores were uniformly distributed in the coatings. No particular porosity increase was detected at the boundaries between superposed coating lines and coating layers. Thus, it is possible to conclude that the porosity in obtained coatings corresponded to the porosity of the first type (intersplat porosity). Low thickness of the coating line per pass allowed to avoid formation of porosity of the second type.

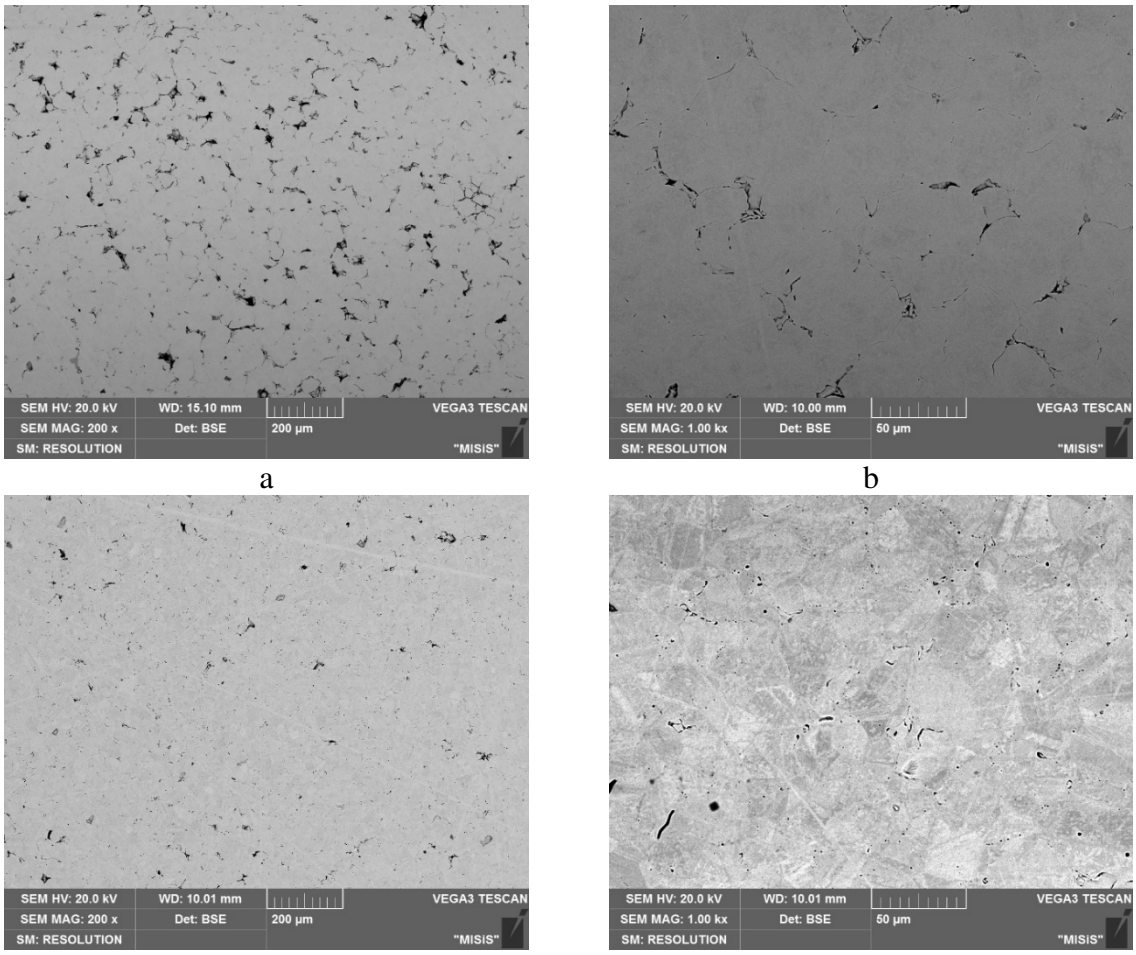

Figure 4 : SEM images of 316L coating microstructure in as-sprayed (a, b) and HIP-treated (c, d) conditions

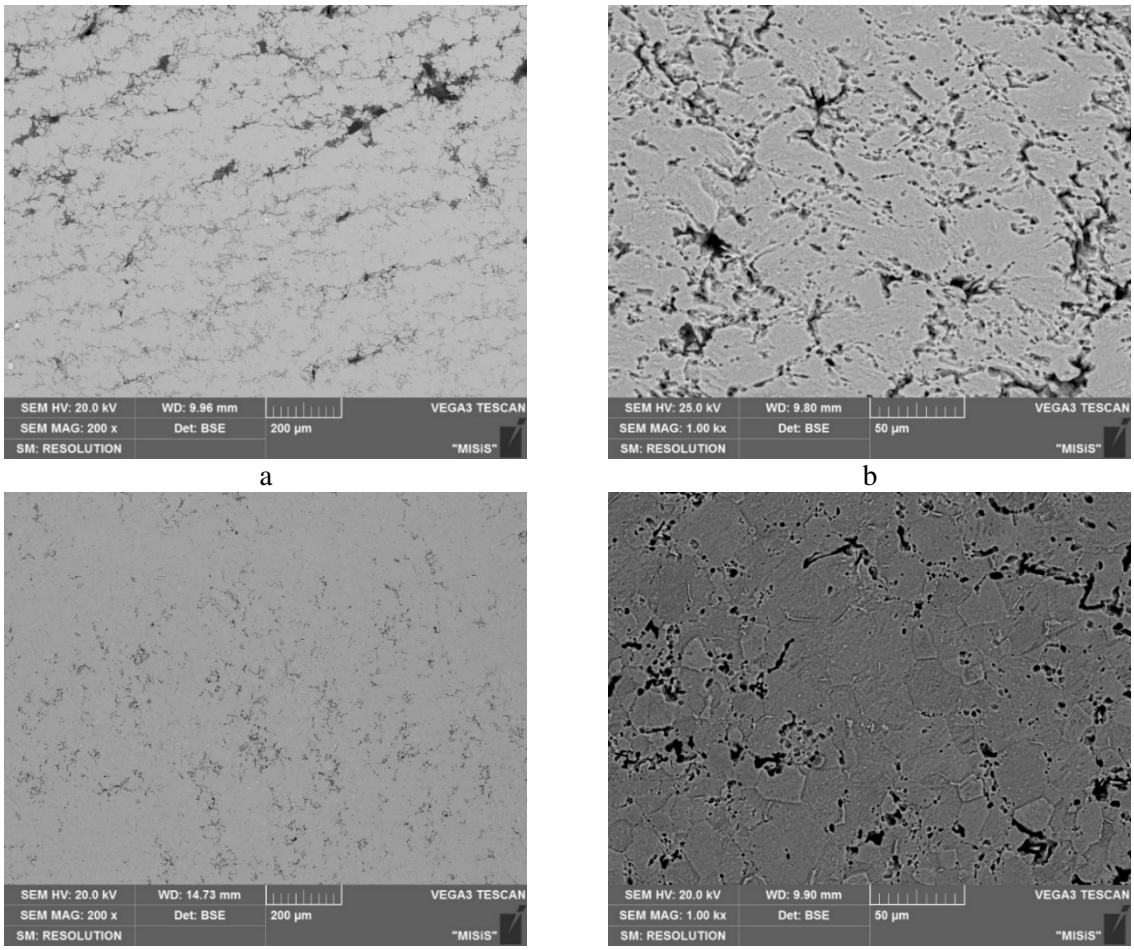

Figure 5 : SEM images of titanium coating microstructure in as-sprayed (a, b) and HIP-treated (c, d) conditions

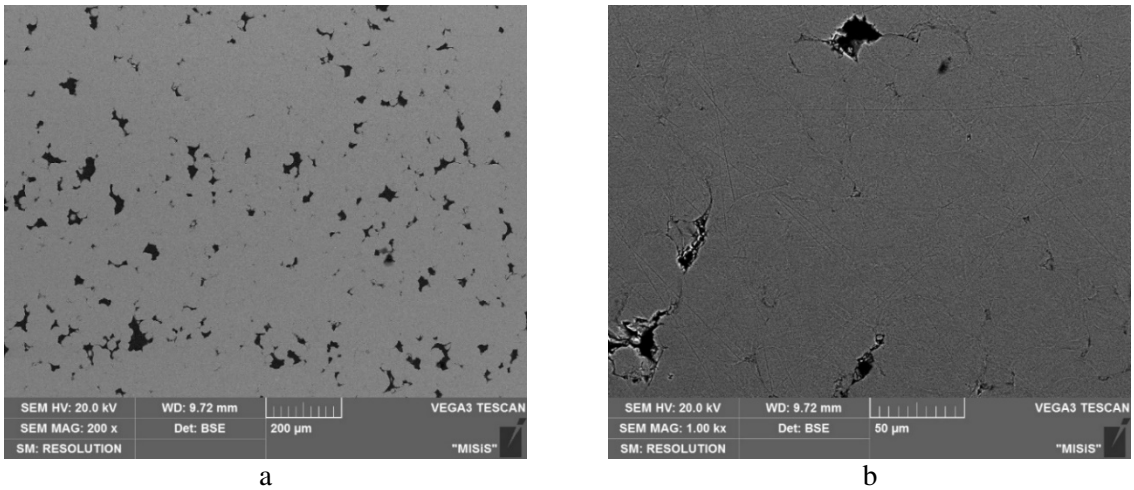

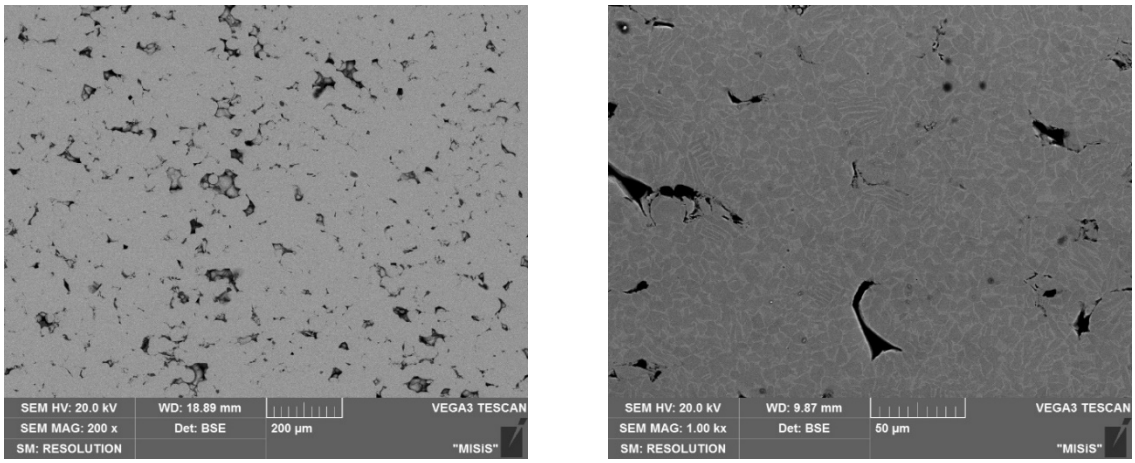

c d

Figure 6 : SEM images of Ti6Al4V coating microstructure in as-sprayed (a, b) and HIP-treated (c, d) conditions

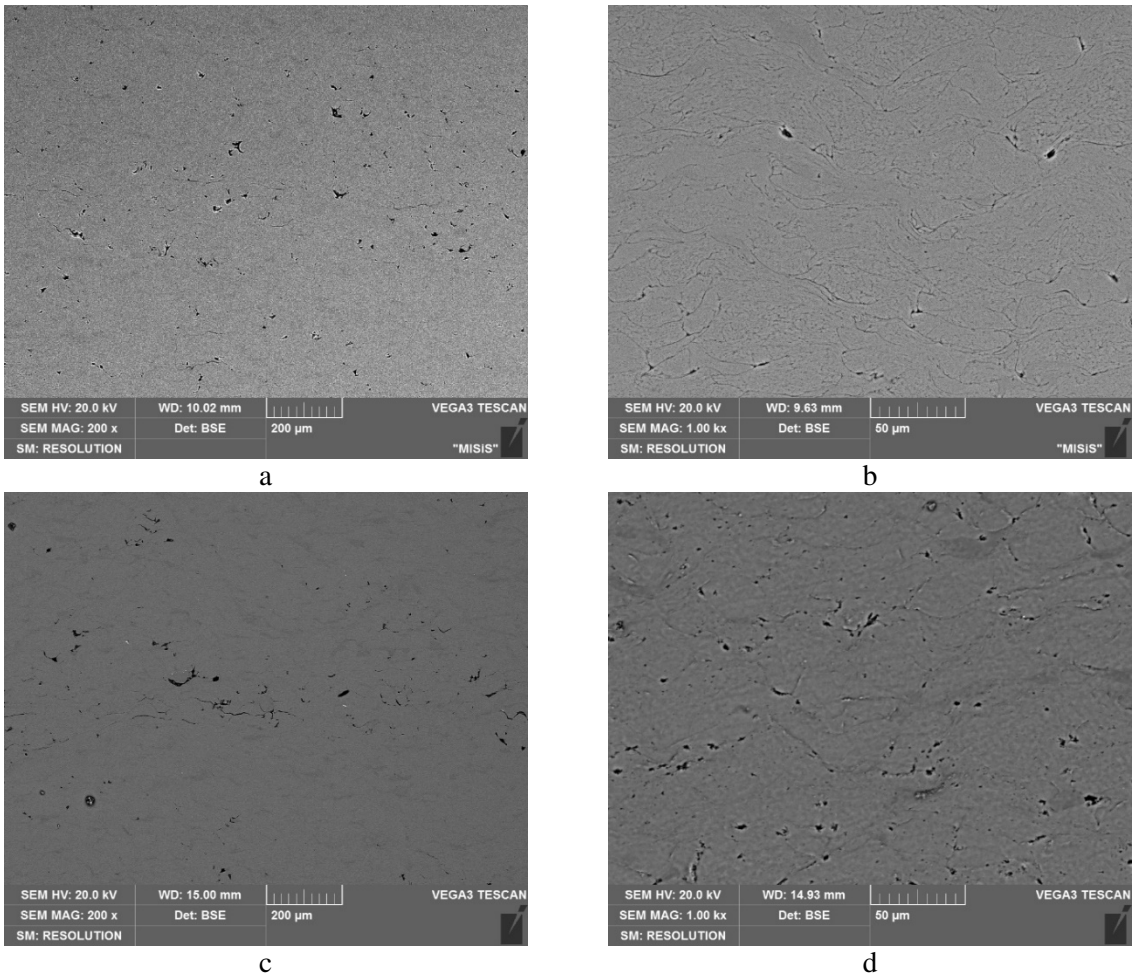

a b

c d

Figure 7 : SEM images of Al-Mg-Sc-Zr coating microstructure in as-sprayed (a, b) and HIP-treated (c, d) conditions

Results of porosity measurements are summarized in Figure 8. On can see that the highest porosity value in as-sprayed conditions were measured for Ti6Al4V coating whereas the Al-

Mg-Sc-Zr had the lowest one. As it was mentioned above, the porosity of the first type strongly depends on the particle deformation pattern. In general, this porosity could be reduced by increase of the particle impact velocity and temperature. In order to characterize the particle impact conditions Assadi et al. [10] introduced η parameter equal to the ratio between the particle impact velocity and the particle critical velocity. Authors stated that in order to maximize the cohesion between splats and the coating density, the value of η parameter should be near 1.5 [9]. Taking into account the pressure and temperature used in experiments and the data provided in [10], it is possible to estimate that the η values for 30 µm particles were equal to ~1.25 for Al-Mg-Sc-Zr alloy, ~1.15 for pure titanium, ~1.1 for 316L stainless steel and 0.85 for Ti6Al4V. One can see that the coating porosity in this study correlates with the η values. Al-Mg-Sc-Zr deposited with the highest η had the lowest porosity. The 316L and pure titanium were sprayed at η close to 1.1 that allowed formation of deposit with moderate porosity. The Ti6Al4 coating sprayed with the lowest η had the highest porosity value. It is important to note that the Ti6Al4 powder contained high number of the particles larger than 30 µm. It is known that under the same spraying parameters the particles larger than 30 µm have smaller impact velocity that diminishes their η value [10]. Taking into account the particle size distribution of Ti6Al4, it is possible to conclude that the significant amount of Ti6Al4 particles impact the surface with η value even lower than 0.85 that leaded to poor splat-splat contact and high intersplat porosity.

The cold spray coating porosity values reported in previous studies of different research groups are also presented in Figure 8. In general, the difference between the results obtained in this study and the literature data could be explained by the spray parameters applied for the coating deposition. For example, higher porosity value of 316L coating (~10%) reported by Adachi and Ueda [32] is explained by lower gas stagnation temperature and pressure. Wang et al [33] performed cold spraying of 316L powder using nitrogen at 1000 °C (versus 650 °C in this study) that allowed producing the coating with the porosity value near 1.8-2.4%. Vo et al. [11] obtained the nitrogen–sprayed Ti6Al4 coatings with porosity near ~8% using similar spraying parameters, but with the finer Ti6Al4 powder. Finally, the pure titanium coatings deposited by Wong et al. [31] using angular titanium powder and the same spray parameters had the porosity near 3.5 %. Increase of the nitrogen temperature up to 1000 °C allowed to produce the pure titanium deposits with the porosity near 1 % [34]. In general, the porosity of as-sprayed deposits obtained in this study was in the range of typical values previously reported for 316L, titanium and Ti6Al4 powders deposited using nitrogen.

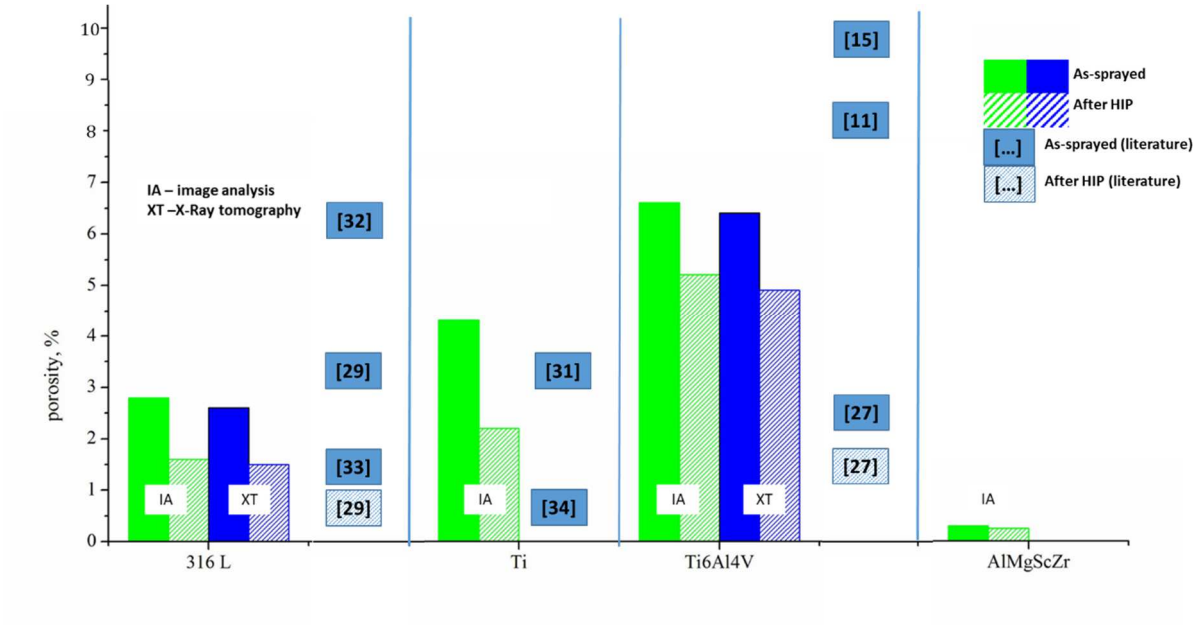

Figure 8 : Results of porosity measurement in as-sprayed and HIP-treated deposits in comparison with typical values available in literature

The cross-section images of the deposits after HIP are also presented in Figures 4-7. SEM observation confirmed that high temperature during HIP process promoted the material diffusion through the splat boundaries. In all HIPed samples the splat boundaries are significantly less distinguishable than in case of as-sprayed samples. Significant grain growth was also observed in the pure titanium and the Ti6Al4V coatings. Same effect was previously reported for titanium cold spray coatings at the similar heat treatment temperatures [11, 13].

The effect of HIP treatment on the porosity of the deposits is summarized in Figure 8. The measurements revealed that the porosities of pure titanium and stainless steel were significantly decreased by capsule-free hot isostatic pressing. However, some residual pores are well detectable by tomography and visible on the coating cross-section on the SEM images. The influence of HIP on initially dense Al-Mg-Sc-Zr samples was not significant due to low initial porosity of the sample at as-sprayed conditions. At the same time the porosity of Ti6Al4V sample after HIP was only 20% lower than for the as-sprayed one. One can conclude, that the densification efficiency of capsule-free HIP treatment applied to the different cold spray coatings significantly depends on the coating material and initial coating porosity. It is known that capsule-free HIP treatment cannot significantly diminish the material porosity if the pores are open (connected with the surface by inside channels) or if the pores are too large. In case of open porosity the pressure increase in the HIP chamber leads to gas pressure increase in the open pores that blocks the process of pore shrinkage. In case of large close pores, significant

amount of residual gas in the pores cannot be absorbed by the metal wall during material shrinkage. During HIP treatment of cold spray deposits both scenarios are possible. For example, the large-scale pores in Ti6Al4V coating containing high amount of residual gas could be also connected with the sample surface. As a consequence, the efficiency of the Ti6Al4V densification by pressurized gas is not high. In case of smaller pores (316L coating) the densification of material by HIP is significantly more efficient.

It important to note that the HIP parameters applied in this study could be not optimal for densification of cold spray deposit. Probably, the increase of the treatment temperature and duration could improve the densification effect. Comparison with the results available in the literature [27, 29] allowed to establish that the densification efficiency of capsule-free HIP was lower than the previously reported ones. For example, Yin et al. [29] succeeded to diminish 316L coating porosity from 3.2% to less than 1%. This difference could be explained by higher HIP parameters applied by Yin et al. in their study. In particular, the treatment was performed at 1000°C during 4 hours at 150 MPa, whereas the treatment duration applied in this study was 2 hours with the similar temperature and pressure. The data reported by Chen et al. [27] for Ti6Al4V coatings could not be used for the proper comparison with the values obtained in this study due to significantly smaller particle size distribution of the powder used for the coating deposition. As a result, the porosity of the coating in as-sprayed conditions obtained by Chen et al. was significantly lower than for the coatings obtained in this study.

Mechanical tests

The values of the tensile strength and strain at failure for as-sprayed and HIP-treated Ti, Ti6Al4V and 316L samples are presented in Figure 9.

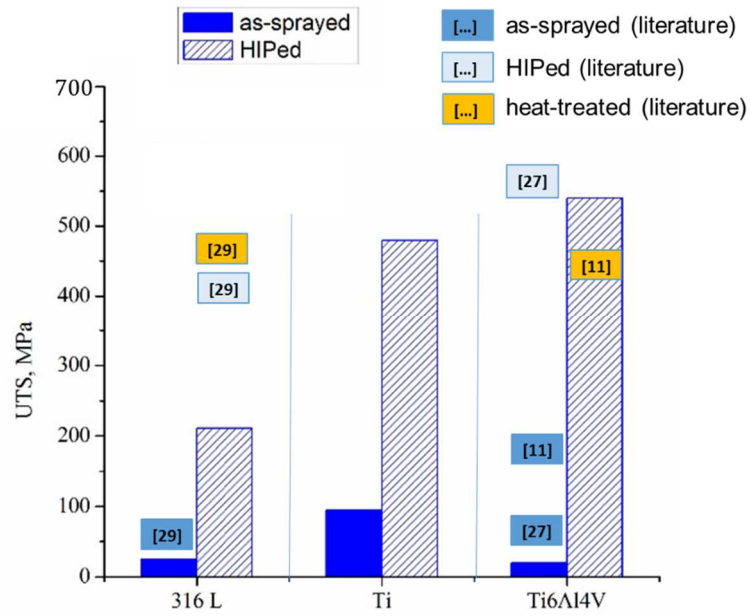

a

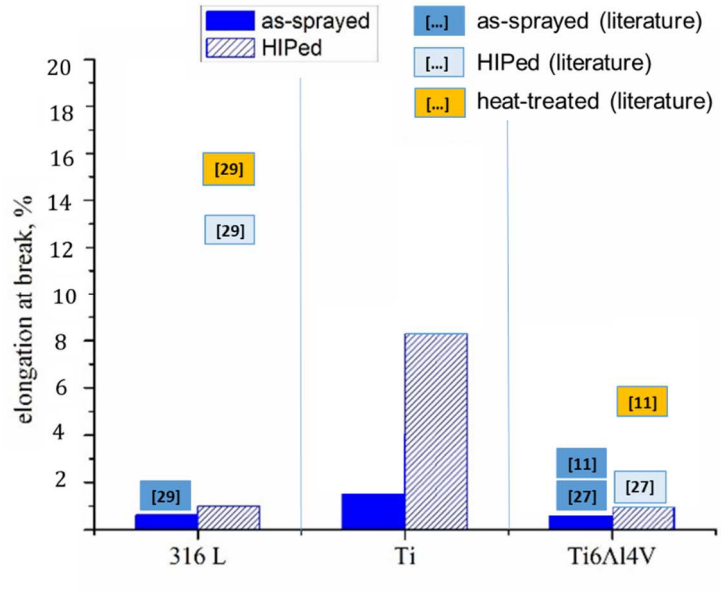

b

Figure 9: Results of tensile strength tests of as-sprayed and HIP-treated cold spray deposits; (a) – ultimate tensile strength, (b) – elongation at break.

All as-sprayed samples exhibited brittle failure with almost no plastic deformation which is typical tensile behavior of cold spray deposits. The best results were obtained with the pure titanium samples where the mean tensile strength and elongation were equal to 90-110 MPa and 2-3 % correspondingly. However these values are significantly lower than for reference bulk titanium (250-400 MPa, 35-55%). The fragile failure of 316L and Ti6Al4V samples occurred at stress near 50 MPa with almost zero elongation that is explained by high sample porosity and low cohesive strength between splats. The obtained results are in good correlation

with the data available in literature. Yin et al [29] also reported almost zero elongation at break with the UTS near 80 MPa for the as-sprayed 316 L deposits sprayed using nitrogen at 1000°C. One can conclude that the deposition at higher temperature (1000°C vs. 650°C in this study) resulting in higher value of η parameter did not allow increasing the UTS of as-sprayed deposits. Similar conclusion could be made for the UTS and elongation at break of Ti6Al4V deposits. Vo et al. [11] performed the deposition at higher gas temperature using finer powder. However, the reported UTS value was close to one obtained in this study.

HIP treatment significantly improved the tensile behavior of all samples. The mean value of tensile strength of titanium samples was equal to 480 MPa that is almost four times higher than the tensile strength of as-sprayed sample. Elongation at break of the samples after HIP raised from 2-3% to 8% that could be explained by material recrystallization and partial porosity elimination. At the same time despite significant improvement of tensile strength the ductility remained significantly lower than the reference value for bulk titanium (~8% vs. 15-20%).

In case of 316L sample the effect of HIP treatment was also clearly seen. Increase of the UTS from ~30 MPa to more than 200 MPa was confirmed with all tensile samples. However in contrast to pure titanium, the improvement of the elongation at break was almost negligible. Comparison with the values provided by Yin et al [29] for the 316L samples after HIP shows that in this study the improvement of UTS and elongation at break by HIP was significantly less efficient than in work of Yin et al. However, as it was mentioned in previous section, the densification efficiency of HIP in the study of Yin et al. was also higher (0.5% of residual porosity vs. 1.5%). Thus, higher sample porosity could explain lower tensile properties measured in this study. It is important to note that Yin et al. reported that the best tensile strength and elongation at break was obtained for the samples annealed in vacuum [29]. Author explain this finding by the influence of the oxide film at the splat interface. This film retained at the particle surfaces in the original inter-particle pore areas, effectively hindering the intimate metallurgical inter-particle bonding even after the pores collapse in HIP [29]. The highest increase of tensile strength was measured within the Ti6Al4V. The UTS value raised more than 10 times (from ~20 MPa to 540 MPa). However the elongation at break was almost the same as for as-sprayed samples. The improvement of the UTS of the samples by hot isostatic pressing could be explained again by the improvement of bonding strength between the splats due to accelerated material diffusion and recrystallization. However, the improved UTS values were lower than the reference values of bulk material due to high residual porosity. Low elongation at break of HIPed samples could also be explained by insufficient material densification.

The tensile properties of the Al-Mg-Sc-Zr after HIP were not evaluated. However, the compressive tests with this coating were performed. The results of the tests are presented in Table 4. All the samples in as-sprayed conditions had cohesive failure during compression. This observation confirmed that the bonding strength between splats is the critical factor determining the mechanical properties of the cold spray deposits in as-sprayed conditions. The HIP treatment allowed to improve the compressive strength. In particular the failure in the samples observed at compressive stress 30% higher than in case of as-sprayed deposit at the strain 27% (15% for as-sprayed deposit). The increase of compressive strength in the samples HIP also can be explained by improvement of the splat bonding due to high temperature and pressure during treatment. However, both as-sprayed and HIP batches of samples had cohesive failure during compression, which indicates on the limited ductility.

Table 4: Compressive properties of AlMgScZr deposits before and after HIP

Condition	Yield strength $\sigma_{0.2}$, MPa	Ultimate compressive strength, σ_{UCS}, MPa	Compressive strain at failure, φ%
As-sprayed	370 ± 8	505 ± 25	15 ± 3.5
After HIP	405 ± 5	645 ± 20	27 ± 3.5

Mechanical test revealed that in general, HIP treatment improved the ultimate tensile strength and the elongation at break of the cold spray deposits. However, the obtained values are significantly smaller than the standard values obtained for bulk materials. It is important to note that this difference could be explained not only by residual porosity in the HIPed deposits but also by the possible formation of brittle phases during material densification. The air trapped inside the closed pores have to absorb by the pore walls during pore shrinkage induced by high pressure. In this case formation of new oxides or other phases could be initiated due to reaction between trapped air and the metallic material of coating. As a result, the increase of the tensile properties due improvement of the contact between splats could be accompanied by embrittlement of the deposits due to ne oxide phase formation. In this regard, the initial porosity of as-sprayed deposit should be considered as important factor, influencing not only the residual porosity after HIP, but also the quantity of new phases formed during pore shrinkage. However, this suggestion should be verified in future studies.

Conclusion

Application of capsule-free hot isostatic pressing for post-treatment of stainless steel, titanium, Ti6Al4V and Al-Mg-Sc-Zr improved the density and mechanical properties of cold-spray deposits. The results of this feasibility study are summarized as follows.

1. The porosity of as-sprayed deposits was significantly different for different materials. The Al-Mg-Sc-Zr deposits had the lowest porosity, whereas the highest porosity was observed for Ti6Al4V coating. These difference could be explained by the spraying parameters applied in this study. In case of deposition of 316L, pure titanium and Ti6Al4V coatings, the spray parameters applied in this study were not capable to provide the particle impact velocity and temperature sufficient for formation of low-porous deposit.
2. In all cases the application of capsule-free HIP for post-treatment of deposits allowed to densify the coating material. However, the residual porosity in HIPed 316L, pure titanium and Ti6Al4V remained elevated. High residual porosity could be explained significant initial porosity of as-sprayed deposits. Also, the applied HIP parameters could be non-optimal for densification of cold spray deposits.
3. HIP treatment enhanced the tensile strength of 316L, pure titanium and Ti6Al4V deposits. The improvement of compression strength was also observed for Al-Mg-Sc-Zr deposit. However, the fragile behavior of all coating were observed during tensile or compressive tests in as-sprayed and HIPed conditions.
4. The detailed study devoted to the optimization of HIP parameters, such as pressure, temperature and duration should be carried out for each given coating material.

Acknowledgments

The study was carried out with the financial support from the Ministry of Science and Higher Education of the Russian Federation within the Increase Competitiveness Program of NUST MISiS (K2-2019-009).

References

1. Papyrin, A, Kosarev, V, Klinkov, S, Alkhimov, A, Fomin, V, Cold Spray Technology, Elsevier Science, Amsterdam, 2007
2. Assadi, H., Gärtner, F., Stoltenhoff, T., Kreye, H. Bonding mechanism in cold gas spraying (2003) Acta Materialia, 51 (15), pp. 4379-4394
3. V.K.Champagne, The cold spray materials deposition process: Fundamentals and applications (2007), pp. 1-362.
4. Maev, R.G and Leshchynsky, V, Introduction to Low Pressure Gas Dynamic Spray: Physics & Technology, Wiley-VCH, Weinheim, 2008
5. J.Vilafuerte, Modern Cold Spray: theory process and applications, Springer International Publishing, Switzerland, 2015
6. Pattison, J., Celotto, S., Morgan, R., Bray, M., O'Neill., W. Cold gas dynamic manufacturing: A non-thermal approach to freeform fabrication (2007) International Journal of Machine Tools and Manufacture, 47 (3-4), pp. 627-634.
7. Schmidt, T, Assadi, H, Gartner, F, Richter, H, Stoltenhoff, T, Kreye, H, Klassen, T, "From Particle Acceleration to Impact and Bonding in Cold Spraying", Journal of Thermal Spray Technology, 18 (2009) pp. 794-808.
8. Hassani-Gangaraj, M., Veysset, D., Champagne, V.K., Nelson, K.A., Schuh, C.A. Adiabatic shear instability is not necessary for adhesion in cold spray (2018) Acta Materialia, 158, pp. 430-439
9. Assadi, H, Schmidt, T, Richter, H, Kliemann, JO, Binder, K, Gartner, F, On parameter selection in cold spraying, Journal of Thermal Spray Technology, 20(6) (2011) 1161-1176
10. H. Assadi, H. Kreye, F. Gärtner, T. Klassen, Cold spraying – A materials perspective, Acta Materialia, 116, (2016), 382-407
11. Vo P, Irissou E, Legoux J-G, Yue S (2013) Mechanical and microstructural

characterization of cold-sprayed Ti-6Al-4V after heat treatment. J Therm Spray Technol 22(6):954–964

12. J. Ridhwan, J.A. Noor, M.S. Zakaria, Z. Zulfattah, M.H.M. Hafidzal, Effect of heat treatment on microstructure and mechanical properties of 6061 aluminum alloy, J. Eng. Technol. 5 (2014) 89–98, https://doi.org/10.4028/www.scientific.net/MSF. 488-489.151.
13. W. Sun, A.-Y. Tan, K. Wu, S. Yin,X. Yang, I. Marinescu, E. Liu, PostProcess Treatments on Supersonic Cold Sprayed Coatings: A Review. Coatings'2020, 10, 123
14. Pierre Coddet, Christophe Verdy, Christian Coddet, Franois Debray, Florence Lecouturier, Mechanical properties of thick 304L stainless steel deposits processed by He cold spray, Surface and Coatings Technology, Volume 277, 2015, Pages 74-80
15. Tan, A.; Lek, J.; Sun, W.; Bhowmik, A.; Marinescu, I.; Song, X.; Zhai, W.; Li, F.; Dong, Z.; Boothroyd, C.; et al. Influence of Particle Velocity When Propelled Using N2 or N2-He Mixed Gas on the Properties of Cold-Sprayed Ti6Al4V Coatings. Coatings 2018, 8, 327
16. Sun, W.; Tan, A.W.Y.; Bhowmik, A.; Marinescu, I.; Song, X.; Zhai, W.; Li, F.; Liu, E. Deposition characteristics of cold sprayed Inconel 718 particles on Inconel 718 substrates with different surface conditions. Mater. Sci. Eng. A 2018, 720, 75–84
17. Yin, S., Cavaliere, P., Aldwell, B., Jenkins, R., Liao, H., Li, W., Lupoi, R. Cold spray additive manufacturing and repair: Fundamentals and applications (2018) Additive Manufacturing, 21, pp. 628-650
18. A. Sova, S. Grigoriev, A. Okunkova, I. Smurov, Cold spray deposition of 316L stainless steel coatings on aluminium surface with following laser post-treatment, Surface and Coating Technology, 2013, vol.235, p. 283-289
19. Yin, S., Jenkins, R., Yan, X., Lupoi, R., Microstructure and mechanical anisotropy of

additively manufactured cold spray copper deposits, (2018) Materials Science and Engineering A, 734, pp. 67-76.

20. Loh, N.L., Sia, K.Y., An overview of hot isostatic pressing (1992) Journal of Materials Processing Tech., 30 (1), pp. 45-65
21. Bocanegra-Bernal, M.H., Hot isostatic pressing (HIP) technology and its applications to metals and ceramics, (2004) Journal of Materials Science, 39 (21), pp. 6399-6420
22. Bonneric, M., Brugger, C., Saintier, N. Effect of hot isostatic pressing on the critical defect size distribution in AlSi7Mg0.6 alloy obtained by selective laser melting (2020) International Journal of Fatigue, 140, art. no. 105797
23. Varela, J., Merino, J., Pickett, C., Abu-Issa, A., Arrieta, E., Murr, L.E., Wicker, R.B., Ahlfors, M., Godfrey, D., Medina, F. Performance characterization of laser powder bed fusion fabricated inconel 718 treated with experimental hot isostatic processing cycles (2020) Journal of Manufacturing and Materials Processing, 4 (3), art. no. 73
24. Leon, A., Levy, G.K., Ron, T., Shirizly, A., Aghion, E. The effect of hot isostatic pressure on the corrosion performance of Ti-6Al-4 V produced by an electron-beam melting additive manufacturing process (2020) Additive Manufacturing, 33, art. no. 101039
25. Khomutov, M., Potapkin, P., Cheverikin, V., Petrovskiy, P., Travyanov, A., Logachev, I., Sova, A., Smurov, I. Effect of hot isostatic pressing on structure and properties of intermetallic NiAl–Cr–Mo alloy produced by selective laser melting (2020) Intermetallics, 120, art. no. 1067667
26. Blose, R. E., Walker, B. H., Walker, R. M., & Froes, S. H. (2006). New opportunities to use cold spray process for applying additive features to titanium alloys. Metal Powder Report, 61(9), 30-37.
27. Chaoyue Chen, Yingchun Xie, Xingchen Yan, Shuo Yin, Hirotaka Fukanuma,

Renzhong Huang, Ruixin Zhao, Jiang Wang, Zhongming Ren, Min Liu, Hanlin Liao, Effect of hot isostatic pressing (HIP) on microstructure and mechanical properties of Ti6Al4V alloy fabricated by cold spray additive manufacturing, Additive Manufacturing, Volume 27, 2019,Pages 595-605

28. Petrovskiy, P., Sova, A., Doubenskaia, M., Smurov, I. Influence of hot isostatic pressing on structure and properties of titanium cold-spray deposits (2019) International Journal of Advanced Manufacturing Technology, 102 (1-4), pp. 819-827
29. Yin, S., Cizek, J., Yan, X., Lupoi, R. Annealing strategies for enhancing mechanical properties of additively manufactured 316L stainless steel deposited by cold spray (2019) Surface and Coatings Technology, 370, pp. 353-361.
30. Petrovskiy, P., Travyanov, A., Cheverikin, V.V., Chereshneva, A.A., Sova, A., Smurov, I. Effect of encapsulated hot isostatic pressing on properties of Ti6Al4V deposits produced by cold spray (2020) International Journal of Advanced Manufacturing Technology, 107 (1-2), pp. 437-449
31. Wong, W., Rezaeian, A., Irissou, E., Legoux, J.G., Yue, S., 2010. Cold Spray Characteristics of Commercially Pure Ti and Ti-6Al-4V. AMR 89–91, 639–644.
32. Adachi, S.; Ueda, N. Effect of Cold-Spray Conditions Using a Nitrogen Propellant Gas on AISI 316L Stainless Steel-Coating Microstructures. Coatings 2017, 7, 87.
33. Wang, Y.; Adrien, J.; Normand, B. Porosity Characterization of Cold Sprayed Stainless Steel Coating Using Three-Dimensional X-ray Microtomography. Coatings 2018, 8, 326.
34. Binder, K., Gottschalk, J., Kollenda, M. et al. Influence of Impact Angle and Gas Temperature on Mechanical Properties of Titanium Cold Spray Deposits. J Therm Spray Tech 20, 234–242 (2011).